

Supporting Information

Motivated water splitting activity of ZnO-based Photoanode by modification of self-doped Lanthanum Ferrite

Xuefeng Long^a, Tong Wang^b, Jun Jin^{*b}, Xinhong Zhao^{*a} and Jiantai Ma^b

[a] Key Laboratory of Low Carbon Energy and Chemical Engineering of Gansu Province. School of Petrochemical Technology, Lanzhou University of Technology, Langongping Road 287, Lanzhou 730050, (P. R. China)

[b] State Key Laboratory of Applied Organic Chemistry (SKLAOC), The Key Laboratory of Catalytic Engineering of Gansu Province, College of Chemistry and Chemical Engineering, Lanzhou University, Lanzhou, Gansu, 730000, (P. R. China)

1、 The relevant calculation equations

Calculation of the Incident photon to current efficiency (IPCE)

IPCE values of the obtained photoanodes could be calculated using the equation below:

$$IPCE(\lambda)(\%) = \left[\frac{J_{mono} \times 1240}{\lambda \times P_{mono}} \right] \times 100\% \quad (1)$$

where J_{mono} is the measured photocurrent density at the specific measurement wavelength (mA cm^{-2}) from the electrochemical workstation, λ is the incident light wavelength (nm) and P_{mono} is the measured irradiance at the specific measurement wavelength (mW m^{-2}).

Calculation of charge carrier density (N_D)

According to the M-S plots, N_D of the photoanode can be calculated using the Mott-Schottky equation

$$N_D = \frac{2}{e\epsilon_0\epsilon} \times \left[\frac{dE}{d\left[\frac{1}{C_s^2}\right]} \right] \quad (2)$$

Where e is electronic charge (1.6×10^{-19} C). ϵ_0 is vacuum permittivity (8.854×10^{-14} F/m), ϵ is the relative permittivity of ZnO (10). C_s is capacitance of the space charge region per unit area of the semiconductor (unit: F cm^{-2}); and E is the applied potential

for M-S curves. What is noteworthy is that the Mott-Schottky equation is derived from the plate electrode, so these calculated the N_D are only used for comparison purposes.

Calculation of the Theoretical maximum photocurrent density (J_{abs})

Theoretical maximum photocurrent density (J_{abs}) is the photocurrent density assuming that all absorbed photons can be converted into current. In the case of J_{abs} , it can be calculated according to the following equation:

$$J_{abs} = \int_{\lambda_1}^{\lambda_2} \frac{\lambda \times (1 - 10^{-A(\lambda)}) \times P(\lambda)}{1240} d(\lambda) \quad (3)$$

where λ and $P(\lambda)$ are the light wavelength (nm) and the corresponding power density ($\text{mW cm}^{-2} \text{ nm}^{-1}$) for the standard solar spectrum AM 1.5G (ASTMG-173-03), $A(\lambda)$ is the absorbance at each wavelength measured by UV-Visible absorption spectra for photoanode.

Calculation of the charge separation efficiency (η_{sep}) and surface charge utilization efficiency ($\eta_{surface}$)

η_{sep} is the yield of photoexcited holes which have migrated to the semiconductor/electrolyte interfaces and $\eta_{surface}$ is the yield of holes that are involved in oxygen evolution reaction after reaching the electrode/electrolyte interfaces. In this work, we chose the widely used Na_2SO_3 as the hole scavenger. η_{sep} and $\eta_{surface}$ were calculated according to the equations, respectively :

$$\eta_{sep} = \frac{J_{\text{Na}_2\text{SO}_3}}{J_{abs}}, \quad \eta_{surface} = \frac{J_{\text{Na}_2\text{SO}_4}}{J_{\text{Na}_2\text{SO}_3}} \quad (4)$$

where $J_{\text{Na}_2\text{SO}_3}$ and $J_{\text{Na}_2\text{SO}_4}$ are the photocurrent densities measured in 0.5 M Na_2SO_4 with and without 0.5 M Na_2SO_3 , respectively.

Calculated photocurrent densities (J_c)

The calculated photocurrent density (J_c) integrated from IPCE spectra was calculated by equation:¹⁻²

$$J_c = \int_{\lambda_1}^{\lambda_2} \frac{\lambda \times IPCE(\lambda) \times P(\lambda)}{1240} d(\lambda) \quad (5)$$

where λ_1 and λ_2 define the integration wavelength range, $IPCE(\lambda)$ is the measured IPCE value as a function of wavelength λ at 1.23 V vs.RHE, λ and $P(\lambda)$ are the light wavelength (nm) and the corresponding power density ($\text{mW cm}^{-2} \text{ nm}^{-1}$) for the standard

solar spectrum AM 1.5G (ASTMG-173–03), respectively.

Semi-quantitative analysis of the atomic ratio

It is recognized that the Element Sensitivity Factor Method is commonly used to semi-quantitatively estimate the relative content of each element. The formula is expressed as: $I = n \times S$, where I refers to the peak area intensity of the characteristic peak, S is called the relative sensitivity factor (RSF) that is the experienced standard constant, and n is the number of atoms of an element per cubic centimeter. Therefore, the relative content of the two elements in a certain sample is:

$$\frac{n_i}{n_j} = \frac{I_i}{S_i} \times \frac{S_j}{I_j} \quad (6)$$

2、 Structural Characterization

The morphologies were examined by a field emission scanning electron microscope (SEM) (HITACHI S-4800, 5 kV). High resolution Transmission electron microscopy TEM (HR-TEM, Tecnai G2Tf20) was conducted to detect the microstructure, combined with an energy dispersive X-ray spectrometer (EDS) for the determination of metal composition. The crystalline phase structure was examined by X-ray diffractometer (Rigaku D/max-2400 power with Cu K α radiation). X-ray photoelectron spectroscopy (XPS) measurements were conducted on a Kratos Axis Ultra DLD using Al K α X-ray source referenced to the C 1s peak (284.6 eV) The light absorption abilities were measured with Ultraviolet–visible absorption spectra (Hitachi U-4000), during which FTO glass as the reference. For steady-state photoluminescence spectra (HITACHI F-7000 equipped with 300 nm pulse laser radiation) was used as measure photoproducted electron-hole pair fluorescent luminescence process at room temperature.

3、 Photoelectrochemical Measurements

All PEC measurements were operated using a conventional three-electrode configuration (platinum foil as counter electrode and Ag/AgCl as reference electrode) in the 0.5 M Na₂SO₄ (pH 6.5) electrolyte, under illuminated using a Xenon lamp source (PLS-SXE300D in Beijing Perfectlight Technology Co., Ltd.). The simulated solar illumination was obtained through an AM 1.5G filter and the light intensity was calibrated to 100 mW cm⁻² by a crystalline silicon solar cell (Photoelectric Instrument

Factory of Beijing Normal University, Model FA-Z). The photocurrents under chopped light irradiation were obtained by linear sweep voltammetry (LSV) at a scan rate of 5 mV/s. Electrochemical impedance spectra (EIS) measurement was collected with amplitude of 5 mV at a bias of 1.2 V vs. RHE with or without solar illumination over a frequency range from 0.1 Hz~100 kHz. The impedance data was fit to an equivalent circuit model using the Zview software (Scribner Associates Inc., USA). Mott-Schottky (MS) spectra were acquired in the potentials range of 0 and 1.2 V vs. RHE in the dark condition at frequency of 1 kHz and scan rate of 20 mV/s. The incident photon-to-current conversion efficiency (IPCE) was measured at 1.23 V vs. RHE by a monochromator between a 300 W Xe lamp as the simulated light source and the PEC cell. The electrode potentials versus the reversible hydrogen electrode (RHE) are converted from the Ag/AgCl electrode using the equation:

$$E_{\text{RHE}} = E_{\text{Ag/AgCl}} + 0.197 + 0.0591\text{pH}.$$

4、 Figures

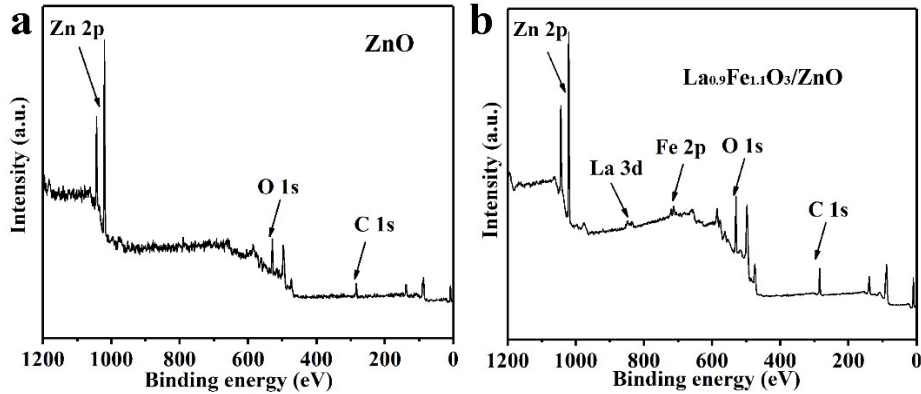


Figure S1. XPS wide scan survey spectra of (a) ZnO and (b) La_{0.9}Fe_{1.1}O₃/ZnO NRs photoanode.

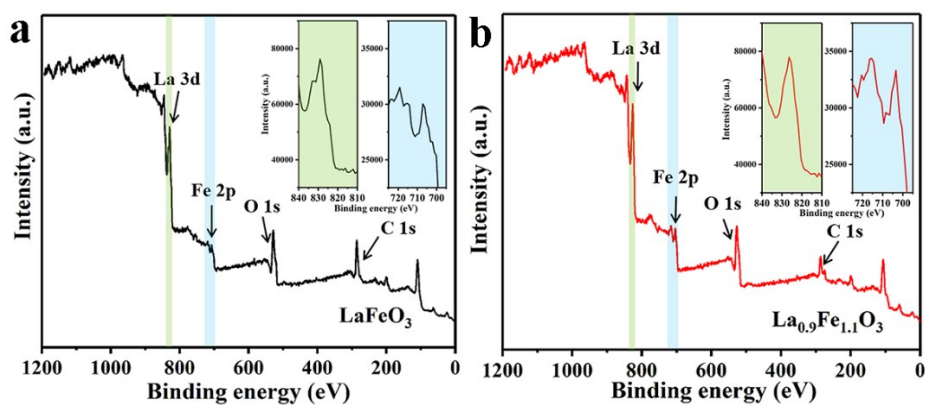


Figure S2. XPS full-spectrum of (a) LaFeO_3 and (b) $\text{La}_{0.9}\text{Fe}_{1.1}\text{O}_3$ powder sample.

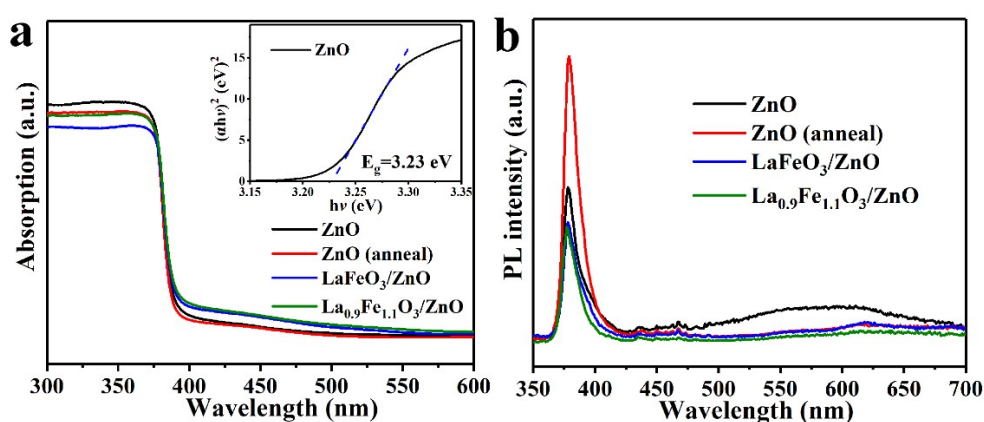


Figure S3. (a) UV-vis absorption spectrum and (b) Photoluminescence spectra (excited with 300 nm pulse laser radiation) of the pristine ZnO NRs, anneal ZnO NRs, $\text{LaFeO}_3/\text{ZnO}$ and $\text{La}_{0.9}\text{Fe}_{1.1}\text{O}_3/\text{ZnO}$ NRs composite photoanode.

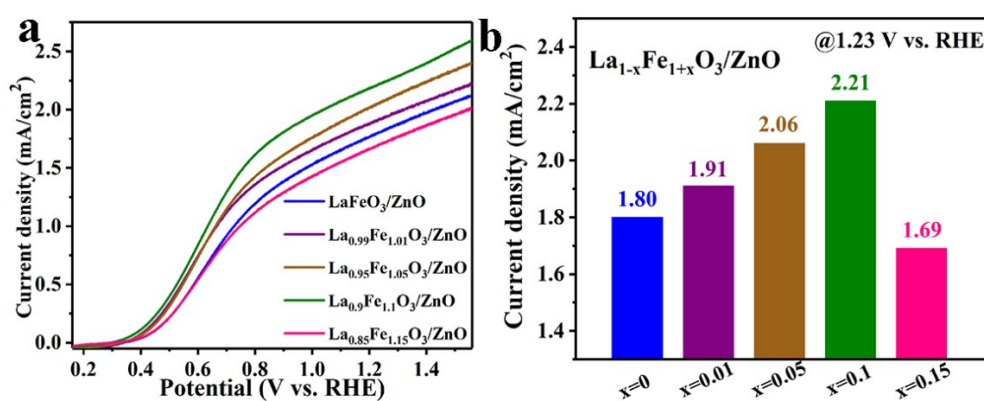


Figure S4. (a) LSV curves and (b) Photocurrent density (@1.23 V vs. RHE) of $\text{La}_{1-x}\text{Fe}_{1+x}\text{O}_3/\text{ZnO}$ NRs photoanodes with different Fe self-doping concentration.

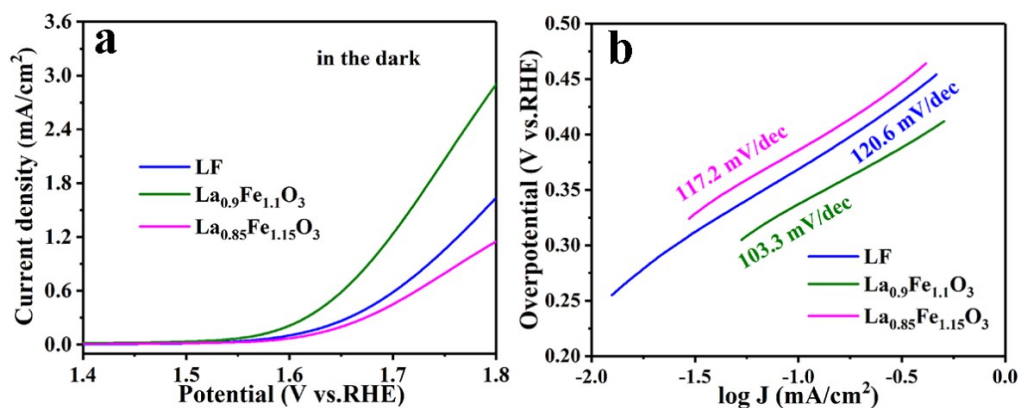


Figure S5. (a) LSV curves and (b) Tafel plots of La_{1-x}Fe_{1+x}O₃ (x=0, 0.1, 0.15) co-catalyst under dark condition.

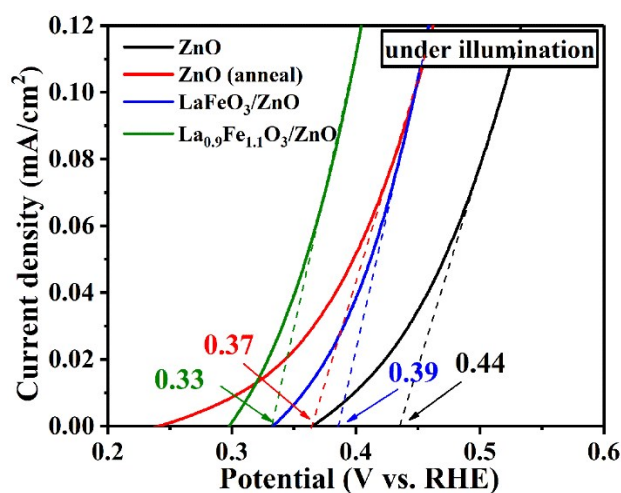


Figure S6. Enlarged view of LSV curves under illumination at low bias potential for confirming onset potentials of all composite photoanodes.

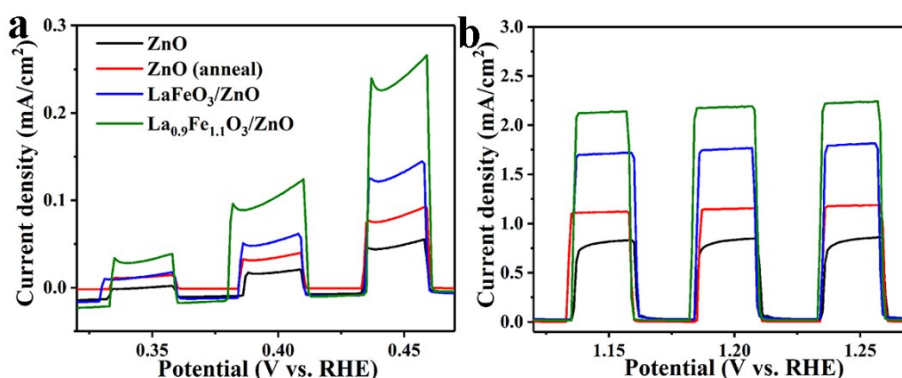


Figure S7. Amplified image of the chopper illumination LSV curve (a) at lower potentials and (b) the higher potentials in Figure 4a of the manuscript.

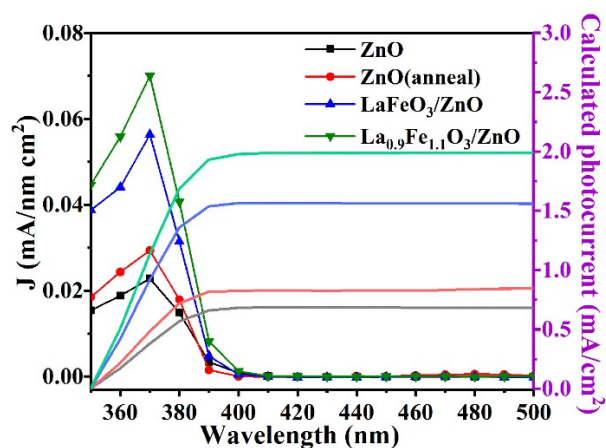


Figure S8. Integral photocurrent density from IPCE measurement at 1.23 V vs.RHE for each photoanodes.

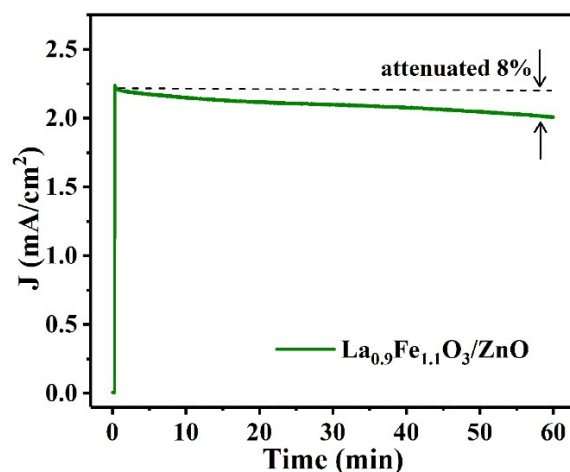


Figure S9. Photocurrent-time curves of the target $\text{La}_{0.9}\text{Fe}_{1.1}\text{O}_3/\text{ZnO}$ NRs photoelectrodes for 3600 s at 1.23 V vs.RHE.

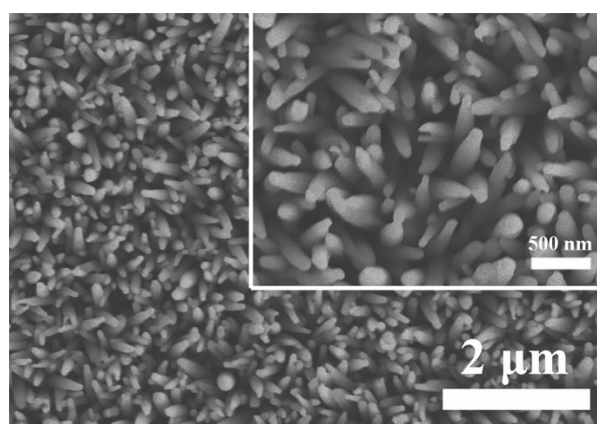


Figure S10. SEM image of $\text{La}_{0.9}\text{Fe}_{1.1}\text{O}_3/\text{ZnO}$ NRs photoanode after the PEC

chronoamperometry testing.

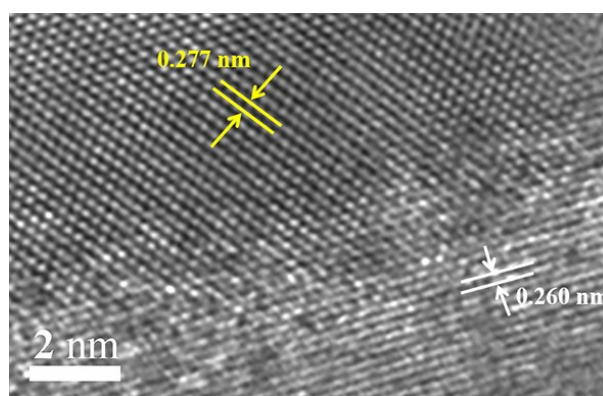


Figure S11. High-Resolution TEM images of the two-phase interface between $\text{La}_{0.9}\text{Fe}_{1.1}\text{O}_3$ and ZnO.

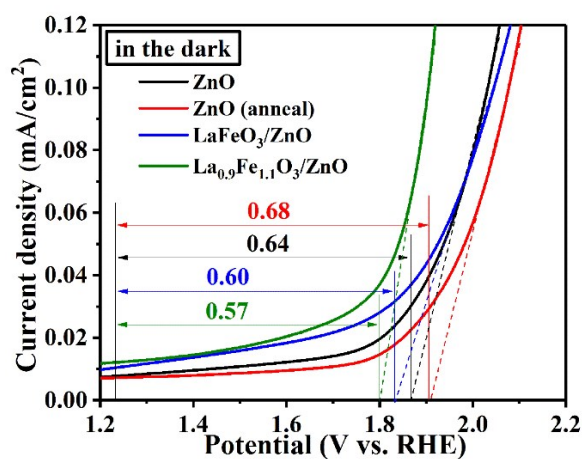


Figure S12. LSV curves in the dark condition for calculating the electrochemical OER kinetic overpotential of each photoanodes.

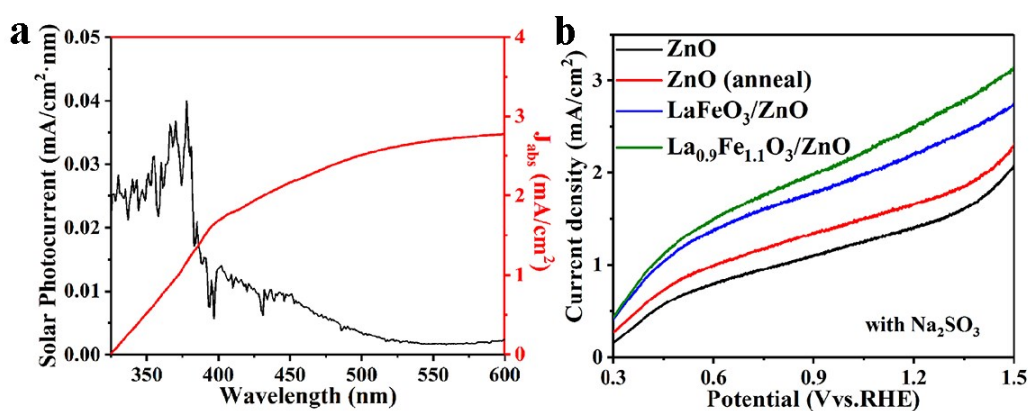


Figure S13. (a) J_{abs} values of ZnO NRs photoanode (assuming 100% absorbed

photon-to-current conversion efficiency for photons). (b) LSV curves under illumination of each photoanode collected in an electrolyte having 0.5 M Na_2SO_3 as hole sacrificial agent (pH 8.5).

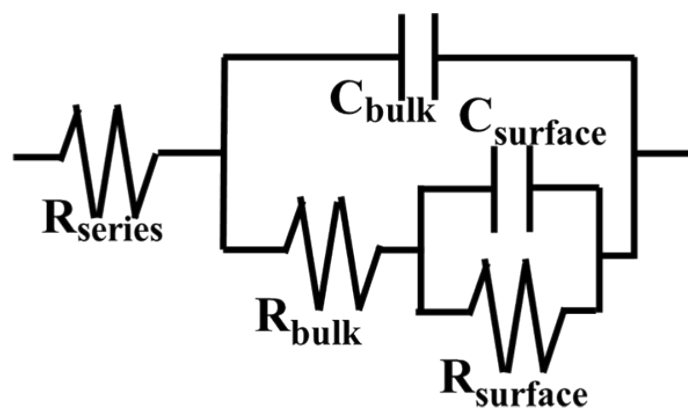


Figure S14. The equivalent circuit models of two-RC-unit.

Table S1. Atomic ratio from the samples surface obtained from XPS.

Sample	Element	Peak Area Intensity	RSF	Atomic ratio (La/Fe)
LaFeO ₃	La 3d	212536.4	9.122	1.0/1.1
	Fe 2p	76753.8	2.957	
La _{0.9} Fe _{1.1} O ₃	La 3d	209517.9	9.122	0.9/1.2
	Fe 2p	91465.2	2.957	

Table S2 Comparison of our photoanode to other ZnO-based composite photoanode

Photoanode material	Electrolyte	Onset potential (V vs.RHE)	Current density (mA/cm ² at 1.23 V vs.RHE)	IPCE value	Ref.
Fe self-doping LaFeO ₃ /ZnO	0.5 M Na ₂ SO ₄	0.33	2.21	50% at 360 nm	This work
LaFeO ₃ /ZnO NRs	0.5 M Na ₂ SO ₄	0.36	1.78	35% at 370 nm	ACS Appl. Mater. Interfaces, 2020, 12, 2452-2459
FeVO ₄ /ZnO NRs	0.5 M Na ₂ SO ₄	0.31	2.05	41% at 370 nm	Appl. Catal. B: Environ. 2019, 257, 117813
NiOOH/ZnW O ₄ /ZnO	0.5 M Na ₂ SO ₄	~0.4	1.7	~46.3% at 350 nm	J. Mater. Chem. A, 2019,7, 2513-2517
ZnO NTs with N-CD embedded ZIF-8	0.5 M Na ₂ SO ₄	~0.1	0.45	~7% at 320 nm	Small 2019, 1902771
ZnO@ZIF-8/67	0.5 M Na ₂ SO ₄	0.3	0.11	1.1% at 600 nm	Applied Surface Science 2018, 448, 254–260

ZnONAs/RGO /ZnIn ₂ S ₄	0.5 M Na ₂ SO ₄	0.35	2.25 mA/cm ² at 2.1 V vs. RHE	--	Nano Energy 2015, 14, 392–400
Co-Pi/ BiVO ₄ /ZnO	0.2 M Na ₂ SO ₄	0.2	~3	~47% at 410 nm	Adv. Energy Mater. 2014, 4, 1301590
ZnO@CoNi- LDH nanoarray	0.5 M Na ₂ SO ₄	0.3	1.5 mA/cm ² at 1.1 V vs. RHE	2.5% at 400 nm	Adv. Funct. Mater. 2014, 24, 580–586
3D-Branched ZnO/CdS NWs	0.5 M Na ₂ S, AM1.5G 70 mW/cm ²	--	3.58 mA/cm ² at 0 V vs. Ag/AgCl	11.5%at 370 nm	Adv. Energy Mater. 2016, 6, 1501459